Published in final edited form as:
Organometallics. 2011 December 12; 30(23): 6482–6489. doi:10.1021/om200908c.

Self-assembly of Cationic, Hetero- or Homo-nuclear Ru(II) Macrocyclic Rectangles and their Photophysical, Electrochemical and Biological Studies

Vaishali Vajpayee[†], **Young Ho Song**[†], **Yoon Jung Yang**[‡], **Se Chan Kang**[*,‡], **Timothy R. Cook**[ζ], **Dong Wook Kim**[±], **Myoung Soo Lah**[±], **In Su Kim**[†], **Ming Wang**[ζ], **Peter J. Stang**[*,ζ], and **Ki-Whan Chi**[*,†]

[†] Department of Chemistry, University of Ulsan, Ulsan 680-749, Republic of Korea.

[‡] Department of Natural Medicine Resources, University of Semyung, Jecheon 390-711, Republic of Korea.

[ζ] Department of Chemistry, University of Utah, Salt Lake City, Utah 84112-0850, U.S.A.

[±] Interdisciplinary School of Green Energy, Ulsan National Institute of Science & Technology, Ulsan, 689-798, Korea.

Abstract

A series of supramolecular rectangles, including two mixed-metal Ru/Pt complexes, have been formed by the coordination-driven self-assembly of a range of arene-Ru "molecular clip" acceptors (**1a**-**1d**) with rigid dipyridyl-based ligands (**2a**-**2d**) over the course of 10 hours in solution. The isolated products were characterized by multinuclear NMR (^{1}H and ^{13}C or ^{31}P), HR-ESI-MS and an X-ray diffraction study to support the ascribed two-component rectangular structures. The rectangles were further characterized by UV-Vis and fluorescence studies. The redox behaviors of rectangles **3ca** and **3da** were also determined using cyclic voltammetry. Additionally, the antitumor activities of the suite of rectangles were determined against various human cancer cell lines and significant activity was shown by complexes **3ca**, **3da**, **3cb**, **3cc** and **3cd**, with IC_{50} values as low as 2.65 μM.

Introduction

Coordination-drive self-assembly is an efficient method to generate supramolecules of a range of shapes and sizes, as evidenced by over two decades of work detailing the formation of squares, triangles, prisms and other 2D and 3D topologies.[1] The synthetic ease and versatility of coordination-driven self-assembly complements the inherent host-guest properties afforded by the nanoscopic voids of the structures, resulting in numerous functional materials which act as sensors, molecular flasks and catalysts.[2-4] While Pd(II) and Pt(II)-based architectures dominate the library of known complexes,[5] the principles and strategies underlying their formation have more recently been applied to incorporate different metal ions. [6] Arene-capped octahedral metal centers are particularly useful in the formation of "molecular clips," which are well-suited for the directional bonding strategy to form rectangles, and prisms. As such, variety of Ru, Rh, Os or Ir sandwich complex

[*]kwchi@ulsan.ac.kr, sckang@semyung.ac.kr, stang@chem.utah.edu.

Supporting Information Available: ^{1}H, ^{13}C NMR and HR-ESI-MS spectra for metalla-rectangles **3**, UV-visible and fluorescence spectra of homometallic rectangles, crystallographic data for the metalla-rectangles **3ab.** This material is available free of charge via the Internet at http://pubs.acs.org.

molecular clips have been utilized for the construction of various 2D and 3D-supramolecules.[7] Supramolecular rectangles are the simplest of these assemblies, requiring only a 1:1 mixture of clip and linear donor. Although simple in design, these structures have shown promising applications as anion sensors and hosts for small molecules.[8] These rectangles typically incorporate a single type of metal ion. However, a second metal can be introduced into the donor component of the self-assembly, potentially imparting unique or enhanced functionalities in the form of mixed-metal, heterometallic scaffolds.

More recently, the biological activity of Ru ions has prompted the synthesis and screening of a number of complexes for their antitumor properties. These studies indicate that Ru-based drugs may provide low non-specific toxicities while maintaining high efficacies relative to platinum-based agents.[9] The mechanism of action of arene-Ru complexes is an active area of study, with evidence that iron mimicking (for eg. when binding with biomolecules) is an important factor.[10] Since these complexes act along a different vector, cell lines which have developed Pt drug resistance remain susceptible to Ru-based treatments.[11] While activity has been seen for small, mononuclear Ru complexes, studies have shown selective cellular uptake and retention of macromolecules inside cancer cells owing to damaged lymphatic drainage.[12] In this context, various nano-prisms have been prepared and initial studies show high cytotoxicity against various human cancer cell lines.[13] We have recently reported the preparation of a series of arene Ru-based rectangles which exhibit significant cytotoxicity against several cancer cell lines.[14] The results suggested that larger metalla-cycles show higher activity over small rectangles, in agreement with the hypothesis that large macromolecules are retained inside cancer cells.

Herein, we report two heterometallic hexanuclear metalla-rectangles which self-assemble upon mixing an arene-Ru acceptor (**1c**, **1d**) with *trans*-[(4-pyridylethynyl)$_2$Pt(PEt$_3$)$_2$] (**2a**) (Scheme 1). This heterometallic rectangle is of special interest for anticancer studies as it possesses two metals ions known to be biologically active. In addition to these heterometallic constructs, a suite of homometallic tetranuclear rectangles are also reported, formed by mixing arene-Ru acceptors **1a-c** with one of three dipyridyl donors, 1,4-di(pyridine-4-yl)buta-1,3-diyne (**2b**), 1,4-di(pyridi-4-yl)benzene (**2c**) and 1,2-di(pyridine-4-yl)ethyne (**2d**) (Scheme 1). The compound numbering used here represents the arene-Ru acceptors as **1a-d**, the dipyridyl donors as **2a-d**, and the resulting self-assemblies as **3**xy where *x* refers to the acceptor and *y* refers to the donor components used. In all cases, two dinuclear Ru precursors react with two dipyridyl ligands, displacing the triflate ligands to yield 4+ triflate salts. The dipyridyl ligands bridge between two Ru acceptors, defining the width of the rectangle, with the height determined by the specific arene-Ru compound used.

Experimental

Material and methods

The chloride analogues of arene-ruthenium acceptors **1a-1d**[8c,11a,11b], their triflate derivatives [8c] and the donors **2a-2d**[1j] were prepared according to literature methods. Deuterated solvents were purchased from Cambridge Isotope Laboratory (Andover, MA). NMR spectra were recorded on a Bruker 300 MHz spectrometer. ^{1}H, ^{13}C and ^{31}P NMR chemical shifts are reported relative to residual solvent (H and C) and H_3PO_4 (P) signals. HR-ESI-Mass spectra were recorded on a Micromass Quattro II triple-quadrupole mass-spectrometer using electrospray ionization and analyzed using the MassLynx software suite. UV-Vis spectra were recorded on Cary 100 Conc. Fluorescence titration studies were carried out on a HORIBA FluoroMax-4 fluorometer. Cyclic valtametry experiments were carried out on Metrohm Autolab B. V.

Cyclic voltammetry

Cyclic voltammetry experiments were carried out with a Metrohm Autolab B. V. potentiostat at room temperature using a 3-electrode cell with platinum disk electrode (AUTOLAB RDE; 3 mm diameter) as the working electrode, platinum sheet auxiliary electrode, and calomel reference electrode. The analyzed compounds were dissolved in dichloromethane (analytical grade) to give a solution containing 5×10^{-4} M of the analytes [chloride analogues of arene-ruthenium acceptors (**1c** and **1d**) and heteronuclear metalla-rectangles (**3ca** and **3da**)] and $0.1 M Bu_4NPF_6$. The redox potentials are given relative to the ferrocene/ ferrocenium reference.

X-ray Structure Determination

A crystal of **3ab** was coated with paratone oil and affixed to a loop. Diffraction data was collected at 193 K with Mo Kα radiation using an X-ray diffraction camera system with an imaging plate equipped with a graphite crystal incident beam monochromator. The RapidAuto software suite[15] was used for data collection and processing. The structure was solved by direct methods and refined by a full-matrix least-squares calculation with the SHELXTL software package.[16] One dipyridyl ligand, one oxalate, two ruthenium atoms, two *p*-cymene ligands and one triflate anion were observed as an asymmetric unit. The other triflate anion was partially identified in the difference Fourier map. The subsequent least-squares refinement on the model containing the partially-identified atoms did not reveal the remaining part of the triflate anion. All non-hydrogen atoms were refined anisotropically; the hydrogen atoms attached to the ligands were assigned isotropic displacement coefficients U(H) = 1.2U (C) and 1.5U (C_{methyl}), and their coordinates were allowed to ride on their respective atoms. The least-squares refinement of the structural model was performed under the geometry constraint AFIX for phenyl and pyridyl parts of the ligand. Additional commands, specifically DFIX, ISOR, and DELU were applied to restrain 1,2 distances, restrain U_{ij} components approximate to isotropic behavior, and enforce a rigid bond restraint, respectively. The final refinement was performed with a modification of the structure factors for the electron densities of the partially identified triflate anion and disordered solvents using the SQUEEZE option of PLATON.[17] Refinement of the structure converged at a final $R1 = 0.0847$, $wR2 = 0.2342$ for 2878 reflections with $I > 2\sigma(I)$; $R1 = 0.1472$, $wR2 = 0.2698$ for all 6210 reflections. The largest difference peak and hole were 1.147 and -0.677 e·Å^{-3}, respectively.

Cancer Cell Growth Inhibition Assay (MTT assay)

Cells were routinely grown in Dulbecco's Modified Eagle Medium (DMEM) supplemented with 10% heat inactivated foetal bovine serum (FBS), 1% penicillin streptomycin at 37 °C and 5% CO_2. The cell suspensions were seeded into 96-well plates at a concentration of 5×10^4 cells per well (90 μL per well and 10 μL sample). MTT ((3-(4,5-Dimethylthiazol-2-yl)-2,5-diphenyltetrazolium bromide) was prepared as a stock solution of 5 mg/mL in phosphate buffer (PBS, pH 7.2) and was filtered. 10 μL of the MTT solution was added to each well. After incubation for 4 h at 37 °C and 5% CO_2, 100 μL of DMSO (dimethylsulfoxide) was added to each well for cell lysis. The plates were read by an enzyme-linked immunosorbent assay (ELISA) reader at 570 nm for absorbance density values to determine the cell viability. The percentage of surviving cells was calculated from the ratio of the absorbance of treated to untreated cells. The half maximal inhibitory concentration (IC_{50}) values for the inhibition of cell growth were determined by fitting the plot of the logarithmic percentage of surviving cells against the logarithm of the drug concentration using a linear regression function.

Stability of rectangles in DMSO—For stability studies, molecular rectangle **3ca** were dissolved in DMSO and the sample was analyzed by ^{1}H NMR spectroscopy immediately after dissolution and after 48 h (supporting information). No change observed even after 48 h, thus attesting the stability of molecular rectangle in DMSO.

General procedure for the synthesis of rectangles (3)—A solution of nitromethane/methanol (1:1, 2 mL) was added to a solid sample of the corresponding arene-ruthenium acceptors (**1a**-**1d**) and 4-dipyridyl donors (**2a**-**2d**) in 1:1 molar ratio. The mixture was stirred at room temperature for 10 hours after which the solution was concentrated and diethyl ether added to precipitate the pure rectangles.

Metalla-rectangle 3ca—Acceptor clip **1c** (9.5 mg, 0.01mmol) and dipyridyl donor **2a** (6.3 mg, 0.01 mmol) were stirred in nitromethane-methanol (1:1, 2 mL) to obtain **3ca**. Isolated yield: 87%. Anal. Calcd for $C_{116}H_{140}F_{12}N_4O_{20}P_4Pt_2Ru_4S_4$: C, 43.74; H, 4.43; N, 1.76. Found: C, 43.60; H, 4.21; N, 1.83. ^{1}H NMR [300 MHz, CD_3NO_2]: δ (ppm) 8.15 (d, *J* = 6.0 Hz, 8H, Hα), 7.20 (s, 4H, Hnq), 7.06 (d, *J* = 6.0 Hz, 8H, Hβ), 5.72 (d, *J* = 6.0 Hz, 8H, Hcym), 5.52 (d, *J* = 6.0 Hz, 8H, Hcym), 2.90 (sept, 4H, C*H*$(CH_3)_2$), 2.14 (m, 36H, CH_3, P($CH_2CH_3)_3$), 1.35 (d, *J* = 6.6 Hz, 24H,CH($CH_3)_2$), 1.20 [t, 36H, P(CH_2CH_3)]; ^{13}C NMR [75 MHz, CD_3NO_2]: δ (ppm) 171.0, 151.0, 139.0, 137.1, 127.1, 123.3, 123.2, 111.6, 103.6, 99.1, 84.0, 83.0, 30.5, 21.0, 16.0, 7.6; ^{31}P {^{1}H} NMR (121 MHz, CD_3NO_2): δ 11.83 (s); MS (ESI) for **3ca** ($C_{116}H_{140}F_{12}N_4O_{20}P_4Pt_2Ru_4S_4$): 1442.9 [M – 2OTf]$^{2+}$, 912.4 [M – 3OTf]$^{3+}$.

Metalla-rectangle 3da—Acceptor clip **1d** (10.6 mg, 0.01 mmol) and dipyridyl donor **2a** (6.3 mg, 0.01 mmol) were stirred in nitromethane-methanol (1:1, 2 mL) to obtain **3da**. Isolated yield: 85%. Anal. Calcd for $C_{132}H_{148}F_{12}N_4O_{20}P_4Pt_2Ru_4S_4$: C, 46.83; H, 4.41; N, 1.66. Found: C, 46.55; H, 4.18; N, 1.59. ^{1}H NMR [300 MHz, CD_3NO_2]: δ (ppm) 8.74 (m, 8H, Hnd), 8.28 (d, *J* = 6.6 Hz, 8H, Hα), 7.94 (m, 8H, Hnd), 6.97 (d, *J* = 6.9 Hz, 8H, Hβ), 5.90 (d, *J* = 6.3 Hz, 8H, Hcym), 5.70 (d, *J* = 6.3 Hz, 8H, Hcym), 3.05 (sept, 4H, CH($CH_3)_2$), 2.25 (s, 12H, CH_3), 2.14 (m, 24H, P($CH_2CH_3)_3$), 1.37 (d, *J* = 6.9Hz, 24H,CH($CH_3)_2$) 1.07 [t, 36H, P(CH_2CH_3)]; ^{13}C NMR [75 MHz, CD_3NO_2]: δ (ppm) 170.6, 152.3, 140.3, 135.2, 134.1, 128.5, 128.4, 108.6, 108.5, 105.1, 100.6, 85.1, 84.0, 31.9, 22.6, 18.0, 8.9; ^{31}P {^{1}H} NMR (121 MHz, CD_3NO_2): δ 11.90 (s); MS (ESI) for **3da** ($C_{132}H_{148}F_{12}N_4O_{20}P_4Pt_2Ru_4S_4$): 1543.2 [M – 2OTf]$^{2+}$, 979.3 [M – 3OTf]$^{3+}$.

Metalla-rectangle 3ab—Acceptor clip **1a** (8.6 mg, 0.01 mmol) and dipyridyl donor **2b** (2.0 mg, 0.01 mmol) were stirred in nitromethane-methanol (1:1, 2 mL) to obtain **3ab**. Isolated yield: 89%. Anal. Calcd for $C_{76}H_{72}F_{12}N_4O_{20}Ru_4S_4.2H_2O$: C, 42.30; H, 3.55; N, 2.60. Found: C, 42.40; H, 3.35; N, 2.38. ^{1}H NMR [300 MHz,CD_3NO_2]: δ (ppm) 8.08 (d, *J* = 6.6 Hz, 8H, Hα), 7.47 (d, *J* = 6.6 Hz, 8H, Hβ), 5.89 (d, *J* = 6.6 Hz, 8H, Hcym), 5.74 (d, *J* = 6.3 Hz, 8H, Hcym), 2.90 (sept, 4H, CH($CH_3)_2$), 2.21 (s, 12H, CH_3), 1.36 (d, *J* = 6.9 Hz, 24H,CH($CH_3)_2$); ^{13}C NMR [75 MHz, CD_3NO_2]: δ (ppm) 172.2, 154.0, 133.6, 129.9, 104.5,99.1, 83.4, 83.1, 81.8, 81.7, 32.5, 22.4, 18.3; MS (ESI) for **3ab** ($C_{76}H_{72}F_{12}N_4O_{20}Ru_4S_4$): 558.4 [M – 3OTf]$^{3+}$.

Metalla-rectangle 3bb—Acceptor clip **1b** (9.1 mg, 0.01 mmol) and dipyridyl donor **2b** (2.0 mg, 0.01 mmol) were stirred in nitromethane-methanol (1:1, 2 mL) to obtain **3bb**. Isolated yield: 85%. Anal. Calcd for $C_{84}H_{76}F_{12}N_4O_{20}Ru_4S_4$: C, 45.40; H, 3.45; N, 2.52. Found: C, 45.13; H, 3.68; N, 2.78. ^{1}H NMR [300 MHz, CD_3NO_2]: δ (ppm) 8.35 (d, *J* = 6.6 Hz, 8H, Hα), 7.52 (d, *J* = 6.6 Hz, 8H, Hβ), 5.97 (d, *J* = 6.6 Hz, 8H, Hcym), 5.76 (d, *J* = 6.0 Hz, 8H, Hcym), 5.72 (s, 4H, Hbq), 2.93 (sept, 4H, CH($CH_3)_2$), 2.23 (s, 12H, CH_3), 1.36 (d, *J* = 6.9Hz, 24H,CH($CH_3)_2$); ^{13}C NMR [75 MHz, CD_3NO_2]: δ (ppm) 185.8, 154.3, 133.4,

129.9, 105.5, 102.8,100.4, 84.8, 83.4, 81.1, 80.4, 32.6, 22.5, 18.3; MS (ESI) for **3bb** ($C_{84}H_{76}F_{12}N_4O_{20}Ru_4S_4$: 591.7 $[M - 3OTf]^{3+}$.

Metalla-rectangle 3cb—Acceptor clip **1c** (9.6 mg, 0.01 mmol) and dipyridyl donor **2b** (2.0 mg, 0.01mmol) were stirred in nitromethane-methanol (1:1, 2 mL) to obtain **3cb**. Isolated yield: 89%. Anal. Calcd for $C_{92}H_{80}F_{12}N_4O_{20}Ru_4S_4.2H_2O$: C, 46.86; H, 3.59; N, 2.38. Found: C, 46.63; H, 3.72; N, 2.04. ^{1}H NMR [300 MHz,CD_3NO_2]: δ (ppm) 8.52 (dd, *J* = 1.2 Hz, *J* = 1.5 Hz, 8H, Hα), 7.45 (dd, *J* = 1.5 Hz, *J* = 1.5 Hz, 8H, Hβ), 7.22 (s, 4H, Hnq), 5.77 (d, *J* = 6.3 Hz, 8H, Hcym), 5.58 (d, *J* = 6.0 Hz, 8H, Hcym), 2.90 (sept, 4H, $CH(CH_3)_2$), 2.15 (s, 12H, CH_3), 1.35 (d, *J* = 6.9Hz, 24H,$CH(CH_3)_2$); ^{13}C NMR [75 MHz, CD_3NO_2]: δ (ppm) 172.5, 153.4, 138.6, 133.1, 129.7, 112.8, 105.3, 100.8, 85.4, 84.5, 81.0, 79.8, 32.1, 22.7, 17.4; MS (ESI) for **3cb** ($C_{92}H_{80}F_{12}N_4O_{20}Ru_4S_4$): 625.1 $[M - 3OTf]^{3+}$.

Metalla-rectangle 3ac—Acceptor clip 1a (8.6 mg, 0.01 mmol) and dipyridyl donor **2c** (2.3 mg, 0.01 mmol) were stirred in nitromethane-methanol (1:1, 2 mL) to obtain **3ac**. Isolated yield: 88%. Anal. Calcd for $C_{80}H_{80}F_{12}N_4O_{20}Ru_4S_4.2H_2O$: C, 43.40; H, 3.82; N, 2.53. Found: C, 43.02; H, 3.91; N, 2.43. ^{1}H NMR [300 MHz, CD_3NO_2]: δ (ppm) 8.08 (d, *J* = 6.6 Hz, 8H, Hα), 7.63 (s, 8H, Hbz), 7.63 (d, *J* = 6.6 Hz, 8H, Hβ), 5.90 (d, *J* = 6.6 Hz, 8H, Hcym), 5.73 (d, *J* = 6.3 Hz, 8H, Hcym), 2.92 (sept, 4H, $CH(CH_3)_2$), 2.21 (s, 12H, CH_3), 1.38 (d, *J* = 6.9Hz, 24H,$CH(CH_3)_2$); ^{13}C NMR [75 MHz, CD_3NO_2]: δ (ppm) 172.41, 153.98, 150.85, 137.90, 129.34, 124.57, 104.33, 99.02, 83.42, 82.85, 32.48, 22.47, 18.30 ; MS (ESI) for **3ac** ($C_{80}H_{80}F_{12}N_4O_{20}Ru_4S_4$): 577.1 $[M - 3OTf]^{3+}$.

Metalla-rectangle 3bc—Acceptor clip **1b** (9.1 mg, 0.01 mmol) and dipyridyl donor **2c** (2.3 mg, 0.01 mmol) were stirred in nitromethane-methanol (1:1, 2 mL) to obtain **3bc**. Isolated yield: 87%. Anal. Calcd for $C_{88}H_{84}F_{12}N_4O_{20}Ru_4S_4$: C, 46.39; H, 3.72; N, 2.46. Found: C, 46.21; H, 3.94; N, 2.51.. ^{1}H NMR [300 MHz, CD_3NO_2]: δ (ppm) 8.36 (d, *J* = 6.6 Hz, 8H, Hα), 7.78 (s, 8H, Hbz), 7.73 (d, *J* = 6.6 Hz, 8H, Hβ), 5.99 (d, *J* = 6.3 Hz, 8H, Hcym), 5.83 (s, 4H, Hbq), 5.77 (d, *J* = 6.3 Hz, 8H, Hcym), 2.96 (sept, 4H, $CH(CH_3)_2$), 2.20 (s, 12H, CH_3), 1.38 (d, *J* = 6.9Hz, 24H,$CH(CH_3)_2$); ^{13}C NMR [75 MHz, CD_3NO_2]: δ (ppm) 185.81, 154.44, 150.82, 138.42, 129.31, 124.56, 105.42, 102.76, 100.20, 84.74, 83.21, 32.58, 22.50, 18.33; MS (ESI) for **3bc** ($C_{88}H_{84}F_{12}N_4O_{20}Ru_4S_4$): 610.4 $[M - 3OTf]^{3+}$.

Metalla-rectangle 3cc—Acceptor clip **1c** (9.6 mg, 0.01 mmol) and dipyridyl donor **2c** (2.3 mg, 0.01 mmol) were stirred in nitromethane-methanol (1:1, 2 mL) to obtain **3cc**. Isolated yield: 90%. Anal. Calcd for $C_{98}H_{88}F_{12}N_4O_{20}Ru_4S_4$: C, 48.48; H, 3.73; N, 2.36. Found: C, 48.20; H, 3.89; N, 2.59. ^{1}H NMR [300 MHz,CD_3NO_2]: δ (ppm) 8.52 (d, *J* = 6.6 Hz, 8H, Hα), 7.70 (s, 8H, Hbz), 7.65 (d, *J* = 6.6 Hz, 8H, Hβ), 7.27 (s, 8H, Hnq), 5.79 (d, *J* = 6.0 Hz, 8H, Hcym), 5.59 (d, *J* = 6.3 Hz, 8H, Hcym), 2.95 (sept, 4H, $CH(CH_3)_2$), 2.16 (s, 12H, CH_3), 1.37 (d, *J* = 6.9Hz, 24H,$CH(CH_3)_2$); ^{13}C NMR [75 MHz, CD_3NO_2]: δ (ppm) 172.79, 153.94, 151.04, 138.87, 129.30, 124.66, 112.77, 105.24, 100.89, 85.81, 84.65, 32.18, 22.43, 17.68; MS (ESI) for **3cc** ($C_{98}H_{88}F_{12}N_4O_{20}Ru_4S_4$): 643.7 $[M - 3OTf]^{3+}$.

Metalla-rectangle 3ad—Acceptor clip **1a** (8.6 mg, 0.01 mmol) and dipyridyl donor **2d** (1.8 mg, 0.01 mmol) were stirred in nitromethane-methanol (1:1, 2 mL) to obtain **3ad**. Isolated yield: 90%. Anal. Calcd for $C_{72}H_{72}F_{12}N_4O_{20}Ru_4S_4.2H_2O$: C, 40.99; H, 3.63; N, 2.66. Found: C, 40.65; H, 3.78; N, 2.71. ^{1}H NMR [300 MHz, CD_3NO_2]: δ (ppm) 8.09, (dd, *J* = 1.2 Hz, *J* = 1.2 Hz, 8H, Hα), 7.52 (d, *J* = 1.5 Hz, *J* = 1.2 Hz, 8H, Hβ), 5.89 (d, *J* = 6.3 Hz, 8H, Hcym), 5.74 (d, *J* = 6.3 Hz, 8H, Hcym), 2.90 (sept, 4H, $CH(CH_3)_2$), 2.17 (s, 12H, CH_3), 1.36 (d, *J* = 6.9Hz, 24H,$CH(CH_3)_2$); ^{13}C NMR [75 MHz, CD_3NO_2]: δ (ppm) 172.34, 153.99, 134.30, 129.63, 104.43, 99.06, 94.2, 83.38, 83.12, 32.47, 22.43, 18.29; MS (ESI) for **3ad** ($C_{72}H_{72}F_{12}N_4O_{20}Ru_4S_4$): 1924.0 $[M - OTf]^{1+}$.

Metalla-rectangle 3bd—Acceptor clip **1b** (9.1 mg, 0.01 mmol) and dipyridyl donor **2d** (1.8 mg, 0.01 mmol) were stirred in nitromethane-methanol (1:1, 2 mL) to obtain **3bd**. Isolated yield: 85%. Anal. Calcd for $C_{80}H_{76}F_{12}N_4O_{20}Ru_4S_4.2H_2O$: C, 43.48; H, 3.65; N, 2.54. Found: C, 43.15; H, 3.78; N, 2.58. ^{1}H NMR [300 MHz, CD_3NO_2]: δ (ppm) 8.36 (dd, *J* = 1.2 Hz, *J* = 1.2 Hz, 8H, Hα), 7.56 (dd, *J* = 1.5 Hz, *J* = 1.5 Hz, 8H, Hβ), 5.96 (d, *J* = 6.3 Hz, 8H, Hcym), 5.76 (s, 4H, Hbq), 5.75 (d, *J* = 6.3 Hz, 8H, Hcym), 2.93 (sept, 4H, $CH(CH_3)_2$), 2.15 (s, 12H, CH_3), 1.36 (d, *J* = 6.9Hz, 24H,$CH(CH_3)_2$); ^{13}C NMR [75 MHz, CD_3NO_2]: δ (ppm) 185.92, 154.36, 133.94, 129.51, 105.82, 102.92, 100.60, 84.72, 83.42, 32.58, 22.49, 18.32; MS (ESI) for **3bd** ($C_{80}H_{76}F_{12}N_4O_{20}Ru_4S_4$): 575.8 $[M - 3OTf]^{3+}$.

Metalla-rectangle 3cd—Acceptor clip **1c** (9.6 mg, 0.01 mmol) and dipyridyl donor **2d** (1.8 mg, 0.01 mmol) were stirred in nitromethane-methanol (1:1, 2 mL) to obtain **3cd**. Isolated yield: 83%. Anal. Calcd for $C_{88}H_{80}F_{12}N_4O_{20}Ru_4S_4.2H_2O$: C, 45.75; H, 3.67; N, 2.43. Found: C, 45.36; H, 3.72; N, 2.41. ^{1}H NMR [300 MHz, CD_3NO_2]: δ (ppm) 8.50 (dd, *J* = 1.2 Hz, *J* = 1.5 Hz, 8H, Hα), 746 (d, *J* = 1.5 Hz, *J* = 1.5 Hz, 8H, Hβ), 7.27 (s, 8H, Hnq), 5.76 (d, *J* = 6.3 Hz, 8H, Hcym), 5.56 (d, *J* = 6.3 Hz, 8H, Hcym), 2.92 (sept, 4H, $CH(CH_3)_2$), 2.15 (s, 12H, CH_3), 1.35 (d, *J* = 6.9Hz, 24H,$CH(CH_3)_2$); ^{13}C NMR [75 MHz, CD_3NO_2]: δ (ppm) 172.44, 153.58, 138.67, 133.79, 129.17, 112.81, 105.42, 100.80, 93.01, 85.41, 84.51, 31.95, 22.41, 17.40; MS (ESI) for **3cd** ($C_{88}H_{80}F_{12}N_4O_{20}Ru_4S_4$): 2124.98 $[M - OTf]^{1+}$, 984.01 $[M - 2OTf]^{2+}$.

Results and Discussion

Synthesis and characterization of heterometallic and homometallic molecular rectangles

The two heterometallic rectangles form upon mixing arene–Ru acceptors **1c** and **1d** with the Pt-based donor (**2a**) in CH_3NO_2/MeOH solution for 10 hours at room temperature (Scheme 1). Precipitation with diethyl ether furnishes **3ca** and **3da** as analytically pure solids. Similarly, the homometallic rectangles also self-assemble upon mixing in CH_3NO_2/MeOH solution. Arene-Ru acceptors **1a**-**1c** were mixed with donors **2b**-**2d** to generate the series of nine rectangles, **3ab**-**3cb**, **3ac**-**3cc**, **3ad**-**3cd**.

The ^{1}H NMR spectra of **3ca** and **3da** are similar, each displaying two doublets corresponding to the pyridyl protons with downfield shifts relative to the free pyridyl ligands. The methyl and isopropyl resonances of the *p*-cymene ligands and ethyl resonances of the phosphines are relatively unaffected by self-assembly; however, the aromatic protons of the *p*-cymene ligands shift downfield. A sharp singlet was observed at δ = 7.20 ppm for the naphthoquinone proton of **3ca** and two multiplets were found at δ = 8.75 and 8.28 ppm for the naphthacenedione protons of **3da**. The ^{31}P NMR spectra of **3ca** and **3da** exhibit sharp singlets at δ 11.83 and 11.90 ppm, respectively, with concomitant Pt satellites, indicative of the symmetric phosphine environment about the Pt center of ligand **2a** (Figure 1). These peaks are unaffected by self-assembly formation. The ^{1}H NMR spectra of the nine homometallic rectangles similarly showed two doublets corresponding to the pyridyl protons of the ligands (see Supporting Information). These signals show downfield shifts relative to the free ligands **2b-d**, due to the loss of electron density upon coordination. The *p*-cymene protons appear as two doublets for **3ab**-**3cd** and the benzoquinone protons for **3bb**, **3bc**, **3bd** and naphthoquinone protons for **3cb**, **3cc** and **3cd** are observed as sharp singlets nearly at δ = 5.76 and 7.27 ppm, respectively.

Electrospray ionization mass spectrometry (ESI-MS) provided further evidence for the formation of rectangles. For the heterometallic rectangles, the ESI mass spectra showed peaks at *m/z* = 1443.2 and 912.4 (for **3ca**) and 1543.7 and 979.3 (for **3da**), corresponding to the consecutive loss of the triflate anions $[M-2CF_3SO_3]^{2+}$ and $[M-3CF_3SO_3]^{3+}$. The peaks were isotopically resolved and matched well with their corresponding theoretical

distribution patterns (see Supporting Information). The homometallic rectangles also provided prominent peaks in their HR-ESI-MS spectra. Peaks were observed for **3ab** at m/z = 558.4 [**3ab** - $3O_3SCF_3^-$]$^{3+}$; for **3bb** at m/z = 591.7 [**3bb** - $3O_3SCF_3^-$]$^{3+}$; for **3cb** at m/z = 625.1 [**3cb** -$3O_3SCF_3^-$]$^{3+}$; for **3ac** at m/z = 557.1 [**3ac** - $3O_3SCF_3$-]$^{3+}$; for **3bc** at m/z = 610.4 [**3bc** - $3O_3SCF_3$-]$^{3+}$; for **3cc** at m/z = 643.7 [**3cc** -$3O_3SCF_3^-$]$^{3+}$; **3ad** at m/z = 1925.0 [**3ad** - $O_3SCF_3^-$]$^{1+}$; for **3bd** at m/z = 575.8 [**3bd** - $3O_3SCF_3^-$]$^{3+}$; for **3cd** at m/z = 989.01 [3**cd** -$2O_3SCF_3^-$]$^{2+}$; for 2124.98 [3**cd** - $O_3SCF_3^-$]$^{1+}$, consistent with the formation of [2 + 2] metalla-rectangles. These observed peaks were isotopically resolved and agreed well with their theoretical isotopic distributions (see Supporting Information).

Single crystals suitable for X-ray diffraction experiments were grown of rectangle **3ab** by the slow diffusion of diethyl ether into a CH_3NO_2/MeOH solution of the isolated product.

The structure of **3ab** (selected bond lengths are summarized in Table 1) approximates a dumbbell-shape with a distance of ~24 Å between the symmetry related methyl groups of the arene ligands (generated from the inversion center, the “diagonal” of the rectangle). The ethynyl moieties of the two dipyridyl donors are bowed inward, with a spacing of ~3.32 Å (C9 – C16; Figure 2) through the center of the rectangle. This close contact suggests intramolecular π-π interactions between the pyridyl donors.

The photophysical properties of the hetero- and homometallic rectangles were investigated using MeOH solutions. The absorption spectra of **3ca** and **3da** (Figure 3, left) are similar, exhibiting high energy bands around 300-360 nm with broad, weak bands extending into the visible wavelengths, ranging from 450-750 nm. These absorption bands are ascribed to a mix of metal-to-ligand (MLCT) or intramolecular charge transfer. Upon excitation at 330 nm, donor **2a** and complexes **3ca** and **3da** are emissive, with bands at 370 and 442 nm (for **2a**), 370 and 390 nm (for **3ca**) and 370, 443, 525 and 560 nm (for **3da**). The emission of **2a** and **3ca** are similar, suggesting that ligand emission dominates the spectrum of the self-assembly. Rectangle **3da** exhibits significantly different emission bands, implicating that the tetracene moiety originating from acceptor **1d** is responsible for the emissive properties of the self-assembly (Figure 3, right) The electronic absorbance and emission spectra of homometallic rectangles **3ab-3cd** were recorded and are summarized in Table 2 (see Supporting Information for spectra). As with their heterometallic counterparts, the absorbance bands for the homometallic assemblies are ascribed to a mix MLCT and intramolecular charge transfer transitions. Upon excitation at 298 nm, the homometallic rectangles **3ab**, **3bb**, **3ac**, **3bc**, **3ad** and **3bd** (the oxalate and benzoquinone-spaced rectangles) showed only weak emissions, likely originating from the electron-rich donor ligands. Rectangles **3cb**, **3cc** and **3cd** could be excited at longer wavelengths due to their more extensive absorption bands, also resulting in emission bands originating from the electron-rich donor ligands. In all cases the metalla-rectangles displayed attenuated emission intensities as compared to the donors **2b**-**2c**, potentially due to photoinduced electron transfer from the acceptor fragments to the donor fragments, as observed for previous arene-Ru systems.[4k]

Cyclic voltammetry (CV) experiments were carried out on **1c**, **1d**, **3ca** and **3da** in dichloromethane solutions containing 0.1 M *n*-Bu_4NPF_6 as a supporting electrolyte. The redox response of **1c** shows an irreversible wave at –1.25 V vs SCE, corresponding to a reduction event. Similarly, **1d** exhibits an onset of cathodic current at –1.34 V; however, this reduction appears to be reversible at a scan rate of 250 mV s^{-1}. The tetracene moiety of **1d** appears to be better suited to accommodate a reduction relative to naphthalene group of **1c**, due to its smaller π-system. As a result, the reduction product of **1d** is stable on the timescale of this CV experiment, resulting in reversible redox behavior. This reduction is likely a Ru(II)/(I) couple, stabilized by molecular orbital contributions from the bridging oxalate-

type ligands. As such, the bridging ligands play a role in stabilizing the reduction products and ultimately in determining the reversibility of the waves.

The redox behaviors of **3ca** and **3da** are markedly different than their corresponding arene-Ru precursors, each showing two dominant reduction events, albeit at different potentials. **3ca** is reduced at –0.95 and –1.35 V, with each reduction appearing reversible across a variety of scan rates between 100 and 250 mV s^{-1}. The redox waves of **3da** are shifted relative to **3ca**, with reductions occurring at –1.35 and –1.70 V. These peaks appear quasi-reversible over a range of scan rates (100 – 250 mV s^{-1}), and may have been affected by an onset of cathodic current as the electrode approached –2.0 V, leading to some decomposition. Since the arene-Ru donors did not show two reversible waves, it is likely that this new reduction event is due to the larger π-system introduced by the Pt-diethynyldipyridyl moieties found in **2a**. With the more extensive orbital manifold associated with self-assembly formation, a second electron can be accommodated and the resulting complexes are stable over the course of the experiments. Since a strong pyridyl donor is expected to increase the energy of the empty e_g set of the low-spin Ru(II) complexes, the reductions at –1.35 and –1.70 V most likely correspond to the waves observed in **1c** and **1d** shifted to more negative potentials, as the Ru centers should be less susceptible to reduction in the presence of strong donors. The first reduction events can then be assigned as originating from the donor fragments. It is unlikely that the Pt(II) centers are so easily reduced, but the extensive π* system involving the ethynyl groups may be the source of the observed waves.

In Vitro Anticancer Activity

The *in vitro* cytotoxicities of the entire suite of hetero- and homometallic rectangles were explored using SK-hep-1 (liver cancer), HeLa (ovary cancer), HCT-15 (colon cancer) and AGS (gastric cancer) human cancer cell lines (Table 3). These cell lines were exposed to increasing concentrations of the metalla-rectangles for 24 h after which a colorimetric MTT assay was performed. These results were compared with the well-known antitumor drugs, cisplatin and doxorubicin. Metalla-rectangles **3ab**, **3bb**, **3ac, 3bc**, **3ad** and **3bd** (the oxalate and benzoquinone-bridged arene-Ru complexes) did not show significant antitumor activity. However, the comparatively larger metalla-rectangles **3ca, 3da** (containing the Pt ligand), **3cb**, **3cc** and **3cd** (the naphthoquinone-bridged arene-Ru) exhibited low micromolar inhibition against all cancer cell lines. The growth inhibition efficacy increased with increasing cavity size and conjugation, and the highest inhibition activity was found for the heterometallic rectangles (Figure 6). In particular, the growth inhibition efficacy of metalla-rectangle **3ca** was higher for all four classes of cancer cells, exceeding that of cisplatin and on the order of doxorubicin.

The growth inhibitory activity data suggest that rectangles possessing large cavity sizes have high antitumor activity with the mixed-metal rectangles containing both Ru and Pt showing the highest activity. While the mechanisms of action of arene-Ru-based complexes are currently poorly understood, it is clear that these complexes have different mechanisms of action than cisplatin; the Ru metallacycles are active against HeLa and AGS cancer cell lines whereas cisplatin showed poor cytotoxicity. Previous studies also indicate that cisplatin and arene-Ru derivatives have different modes of action on cell-cycle regulation. During apoptosis, arene-Ru derivatives arrest the cell cycle in G1-phase,[11b] whereas cisplatin affects cancer cells during the G2-phase.[18] Also extended conjugation and increased nuclearity appears to have an impact on the activity of the metallacyclic complexes towards cancer cell lines, as reflecting from the lowest IC_{50} values of **3ca** and **3da**.

Conclusion

In conclusion, we have described the synthesis and characterization of a suite of hetero- and homo-metallic rectangles which self-assemble from mixtures of arene-Ru based acceptors and 4-dipyridyl donors. These rectangles were characterized by multinuclear NMR (^{1}H and ^{13}C or ^{31}P NMR), HR-ESI-MS analysis. The solid state structure of **3ab** was determined by a single crystal X-ray diffraction study, confirming the rectangular structure assigned to these complexes. The absorbance and fluorescence properties for all metalla-rectangles were measured, indicating MLCT and intramolecular charge transfer absorption bands tailing far into the visible region, and emission bands arising from the donor and acceptor fragments. The electrochemical behaviour for the heterometallic rectangles has been studied. The arene-Ru acceptors show reduction events assigned to the Ru(II)/Ru(I) couple, stabilized by the bridging naphthalene or tetracene-based ligands. The more stabilizing tetracene ligand imparts reversibility to **1d**, while the reduction of **1c** is irreversible. Upon self-assembly formation, the resulting rectangles (**3ca** and **3da**) both exhibit two reduction waves. One wave is ascribed to Ru reduction, as observed in the precursors, with the other arising from the incorporation of the Pt-diethynyl-dipyridyl ligands. Both waves have a large degree of reversibility for both complexes; however, the return current for **3da** is slightly attenuated. The anti-tumor activities of the rectangles were evaluated against SK-hep-1, HeLa, HCT-15 and AGS human cancer cell lines. Preliminary results indicate that the larger metalla-rectangles possessed comparative high antitumor activity, on the order of that of cisplatin and doxorubicin. A detailed study on the mode of action as well as cellular uptake of metalla-rectangles is underway.

Supplementary Material

Refer to Web version on PubMed Central for supplementary material.

Acknowledgments

This work was supported by the World Class University (WCU) program (R33-2008-000-10003) and Priority Research Centers program (2009-0093818) through the National Research Foundation of Korea (NRF) funded by the Ministry of Education, Science and Technology. P. J. S. thanks the NIH (GM-57052) for financial support.

References

1. a Lehn JM. Science. 1985; 227:849–856. [PubMed: 17821215] b Lehn JM. Angew. Chem. 1990; 102:1347–1362.c Stang PJ, Olenyuk B. Acc. Chem. Res. 1997; 30:502–518.d Leininger S, Olenyuk B, Stang PJ. Chem. Rev. 2000; 100:853–908. [PubMed: 11749254] e Seidel SR, Stang PJ. Acc. Chem. Res. 2002; 35:972–983. [PubMed: 12437322] f Jones CJ. Chem. Soc. Rev. 1998; 27:289–299.g Holliday BJ, Mirkin CA. Angew. Chem., Int. Ed. 2001; 40:2022–2043.h Oliver CG, Ulman PA, Wiester MJ, Mirkin CA. Acc. Chem. Res. 2008; 41:1618–1629. [PubMed: 18642933] i Chakrabarty R, Mukherjee PS, Stang PJ. Chem. Rev. 2011 dx.doi.org/10.1021/cr200077m. j Lehn, J-M. Supramolecular Chemistry, Concepts and Perspectives. VCH; New York: 1995. k Nehete UN, Anantharaman G, Chandrasekhar V, Murugavel R, Roesky HW, Vidovic D, Magull J, Samwer K, Sass BJ. Angew. Chem., Int. Ed. 2004; 43:3832–3835.l Badjic JD, Nelson A, Cantrill SJ, Turnbull WB, Stoddart JF. Acc. Chem. Res. 2005; 38:723–732. [PubMed: 16171315] m Dash BP, Satapathy R, Maguire JA, Hosmane NS. Org. Lett. 2008; 10:2247–2250. [PubMed: 18465864] n Nitschke JR. Acc. Chem. Res. 2007; 40:103–112. [PubMed: 17309191]

2. a Fujita M, Tominaga M, Hori A, Therrien B. Acc. Chem. Res. 2005; 38:369–378. [PubMed: 15835883] b Fujita M. Chem. Soc. Rev. 1998; 27:417–425.c Rang A, Engeser M, Maier NM, Nieger M, Lindner W, Schalley CA. Chem. Eur. J. 2008; 14:3855–3859. [PubMed: 18351704] d Peinador C, Pía E, Blanco V, García MD, Quintela JM. Org. Lett. 2010; 12:1380–1383. [PubMed: 20218642] e Zheng YR, Yang HB, Northrop BH, Ghosh K, Stang PJ. Inorg. Chem. 2008; 47:4706–4711. [PubMed: 18433099] f Stang PJ, Olenyuk B, Fan J, Arif AM. Organometallics. 1996;

15:904–908.g Stang PJ, Chen K, Arif AM. J. Am. Chem. Soc. 1995; 117:6273–6283.h Schweiger M, Seidel R, Arif AM, Stang PJ. Inorg. Chem. 2002; 41:2556–2559. [PubMed: 11978126] i Fujita M, Sasaki O, Mitsuhashi T, Fujita T, Yazaki J, Yamaguchi K, Ogura K. Chem. Commun. 1996:1535–1536.j Das N, Ghosh A, Singh OM, Stang PJ. Org. Lett. 2006; 8:1701–1704. [PubMed: 16597145] k Ghosh S, Chakrabarty R, Mukherjee PS. Inorg. Chem. 2009; 48:549–556. [PubMed: 19072218] l Bar AK, Chakrabarty R, Mostafa G, Mukherjee PS. Angew. Chem., Int. Ed. 2008; 47:8455–8459.m Kawamichi T, Kodama T, Kawano M, Fujita M. Angew. Chem., Int. Ed. 2008; 47:8030–8032.n Jude H, Disteldorf H, Fischer S, Wedge T, Hawkridge AM, Arif AM, Hawthorne MF, Muddiman DC, Stang PJ. J. Am. Chem. Soc. 2005; 127:12131–12139. [PubMed: 16117555] o Whiteford JA, Stang PJ, Huang SD. Inorg. Chem. 1998; 37:5595–5601. [PubMed: 11670707] p Schnebeck RD, Randaccio L, Zangrando E, Lippert P. Angew. Chem., Int. Ed. 1998; 37:119–121.q Fan J, Whiteford JA, Olenyuk B, Levin MD, Stang PJ. J. Am. Chem. Soc. 1999; 121:2741–2752.r Drain CM, Lehn JMJ. Chem. Soc., Chem. Commun. 1994:2313–2315.s Ikeda A, Udzu H, Zhong Z, Shinkai S, Sakamoto S, Yamaguchi K. J. Am. Chem. Soc. 2001; 123:3872–3877. [PubMed: 11457136]

3. a Hou J–L, Ajami D, Rebek J Jr. J. Am. Chem. Soc. 2008; 130:7810–7811. [PubMed: 18507459] b Yoshizawa M, Klosterman JK, Fujita M. Angew. Chem., Int. Ed. 2009; 48:3418–3438.c Caulder DL, Powers RE, Parac TN, Raymond KN. Angew. Chem., Int. Ed. 1998; 37:1840–1842.d Umemoto K, Yamaguchi K, Fujita M. J. Am. Chem. Soc. 2000; 122:7150–7151.e Kishi N, Li Z, Yoza K, Akita M, Yoshizawa M. J. Am. Chem. Soc. 2011; 133:11438–11441. [PubMed: 21707060] f Fujita M, Aoyagi M, Ibukuro F, Ogura K, Yamaguchi K. J. Am. Chem. Soc. 1998; 120:611–612.
4. a Yao L-Y, Qin L, Xie T-Z, Li Y-Z, Yu S-Y. Inorg. Chem. 2011; 50:6055–6062. [PubMed: 21657232] b Bondy CR, Gale PA, Loeb SJ. J. Am. Chem. Soc. 2004; 126:5030–5031. [PubMed: 15099061] c Vega IED, Gale PA, Light ME, Loeb SJ. Chem. Commun. 2005:4913–4915.d Yu S-Y, Huang H-P, Li S-H, Jiao Q, Li Y-Z, Wu B, Sei Y, Yamguchi K, Pan YJ, Ma H-W. Inorg. Chem. 2005; 44:9471–9488. [PubMed: 16323935] e Ning G-H, Yao L-Y, Liu L-X, Xie T-Z, Li Y-Z, Qin Y, Pan Y-J, Yu S-Y. Inorg. Chem. 2010; 49:7783–7792. [PubMed: 20690696] f Shanmugam S, Bar AK, Chi K-W, Mukherjee PS. Organometallics. 2011; 29:2971–2980.g Qin Z, Jennings MS, Puddephatt RJ. Inorg. Chem. 2003; 42:1956–1965. [PubMed: 12639130] h Sun S-S, Lees AJ. Chem. Commun. 2000:1687–1688.i Beer PD, Szemes F, Balzani V, Sala CM, Drew MGB, Dent SW, Maestri M. J. Am. Chem. Soc. 1997; 119:11864–11875.j Qin Z, Jennings MC, Puddephatt RJ. Chem. Commun. 2002:354–355.k Vajpayee V, Kim H, Mishra A, Mukherjee PS, Stang PJ, Lee MH, Kim HK, Chi K-W. Dalton Trans. 2011; 40:3112–3115. [PubMed: 21321785]
5. a Qin Z, Jennings MC, Puddephatt RJ. Chem. Commun. 2001:2676–2677.b Sautter A, Schmid DG, Jung G, Wurthner F. J. Am. Chem. Soc. 2001; 123:5424–5430. [PubMed: 11389622] c Schnebeck R-D, Freisinger E, Glahe F, Lippert B. J. Am. Chem. Soc. 2000; 122:1381–1390.d Hall J, Loeb SJ, Shimizu GKH, Yap GPA. Angew. Chem., Int. Ed. 1998; 37:121–123.e Goeb S, Prusakova V, Wang X, Vèzinat A, Sallè M. Chem. Commun. 2011; 47:4397–4399.f Lusby PJ, Müller P, Pike SJ, Slawin AMZ. J. Am. Chem. Soc. 2009; 131:16398–16400. [PubMed: 19856967] g Ghosh S, Chakrabarty R, Mukherjee PS. Dalton Trans. 2008:1850–1856. [PubMed: 18369491]
6. a Dinolfo PH, Williams ME, Stern CL, Hupp JT. J. Am. Chem. Soc. 2004; 126:12989–13001. [PubMed: 15469297] b Benkstein KD, Hupp JT, Stern CL. Angew. Chem., Int. Ed. 2000; 39:2891–2893.c Dinolfo PH, Hupp JT. Chem. Mater. 2001; 13:3113–3125.d Yu W-B, Han Y-F, Lin Y-J, Jin G-X. Organometallics. 2010; 29:2827–2830.e Zhang W-Z, Han Y-F, Lin Y-J, Jin G-X. Dalton Trans. 2009:8426–8431. [PubMed: 19789798] f Wang M, Vajpayee V, Shanmugaraju S, Zheng Y-R, Zhao Z, Kim H, Mukherjee PS, Chi K-W, Stang PJ. Inorg. Chem. 2011; 50:1506–1512. [PubMed: 21214171]
7. a Han Y-F, Jia W-G, Yu W-B, Jin G-X. Chem. Soc. Rev. 2009:3419–3434. [PubMed: 20449060] b Boyer JL, Kuhlman ML, Rauchfuss TB. Acc. Chem. Res. 2007; 40:233–242. [PubMed: 17284016] c Barry NPE, Furrer J, Freudenreich J, Süss-Fink G, Therrien B. Eur. J. Inorg. Chem. 2010:725–728.d Han Y-F, Lin Y-J, Jia W-G, Wang G-L, Jin G-X. Chem. Commun. 2008:1807–1809.e Mattsson J, Zava O, Renfrew AK, Sei Y, Yamaguchi K, Dyson PJ, Therrien B. Dalton Trans. 2010; 39:8248–8255. [PubMed: 20689885] f Barry NPE, Edafe F, Dyson PJ, Therrien B. Dalton Trans. 2010; 39:2816–2820. [PubMed: 20200707]
8. a Piotrowski H, Polborn K, Hilt G, Severin K. J. Am. Chem. Soc. 2001; 123:2699–2700. [PubMed: 11456954] b Han Y-F, Jia W-G, Lin Y-J, Jin G-X. Angew. Chem. Int. Ed. 2009; 48:6234–6238.c

Yan H, Süss-Fink G, Neels A, Stoeckli-Evans H. J. Chem. Soc. Dalton Trans. 1997:4345–4350.d Han Y-F, Lin Y-J, Jia L-H, Weng W-G, Jin G-X. Organometallics. 2007; 26:5848–5853.e Jia W-G, Han Y-F, Lin Y-J, Weng L-H, Jin G-X. Organometallics. 2009; 28:3459–3464.f Linares F, Galindo MA, Galli S, Romero MA, Navarro JAR, Barea E. Inorg. Chem. 2009; 48:7413–7420. [PubMed: 19586019] g Zhang W-Z, Han Y-F, Lin Y-J, Jin G-X. Organometallics. 2010; 29:2842–2849.h Vajpayee V, Song YH, Lee MH, Kim H, Wang M, Stang PJ, Whan K-W. Chem. Eur. J. 2011; 17:7837–7844. [PubMed: 21611989]

9. a Dyson PJ, Sava G. Dalton Trans. 2006:1929–1933. [PubMed: 16609762] b Magennis SW, Habtemariam A, Novakova O, Henry JB, Meier S, Parsons S, Oswald IDH, Brabec V, Sadler PJ. Inorg. Chem. 2007; 46:5059–5068. [PubMed: 17497848] c Yan YK, Melchart M, Habtemariam A, Sadler PJ. Chem. Commun. 2005:4764–4776.
10. Allardyce CS, Dyson PJ. Plat. Met. Rev. 2001; 45:62–69.
11. a Therrien B, Süss-Fink G, Govindaswamy P, Renfrew AK, Dyson PJ. Angew. Chem., Int. Ed. 2008; 47:3773–3776.b Vajpayee V, Yang YJ, Kang SC, Kim H, Kim IS, Wang M, Stang P, Chi K-W. Chem. Commun. 2011; 47:5184–5186.c Zava O, Mattsson J, Dyson PJ, Therrien B. Chem.–Eur. J. 2010; 16:1428–1431. [PubMed: 20033971]
12. a Matsumura Y, Maeda H. Cancer. Res. 1986; 46:6387–6392. [PubMed: 2946403] b Maeda H. Advan. Enzyme Regul. 2001; 41:189–207. [PubMed: 11384745]
13. a Barry NPE, Zava O, Furrer J, Dyson PJ, Therrien B. Dalton Trans. 2010; 39:5272–5277. [PubMed: 20442944] b Pitto-Barry A, Barry NPE, Zava O, Deschenaux R, Dyson PJ. Chem.–Eur. J. 2011; 17:1966–1971. [PubMed: 21274948] c Pitto-Barry A, Barry NPE, Zava O, Deschenaux R, Therrien B. Chem. –Asian J. 2011; 6:1595–1603. [PubMed: 21626704] d Barry NPE, Zava O, Dyson PJ, Therrien B. Chem.–Eur. J. 2011; 17:9669–9677. [PubMed: 21735491]
14. Vajpayee V, Song YH, Yang YJ, Kang S, Kim H, Kim IS, Wang M, Stang PJ, Chi K–W. Organometallics. 2011; 30:3242–3245. [PubMed: 21779140]
15. Rapid Auto software. R-Axis series, Cat. No. 9220B101. Rigaku Corporation;
16. Sheldrick, SL. Crystal Structure Analysis Package. Bruker Analytical X-Ray; Madison, WI, USA: 1997. SHELXTL-PLUS.
17. PLATON program. Spek AL. Acta Crystallogr. Sect. A. 1990; 46:194.
18. Kisova A, Zerzankova L, Habtemariam A, Sadler PJ, Brabec V, Kasparkova J. Mol. Pharmaceutics. 2011; 8:949–957.

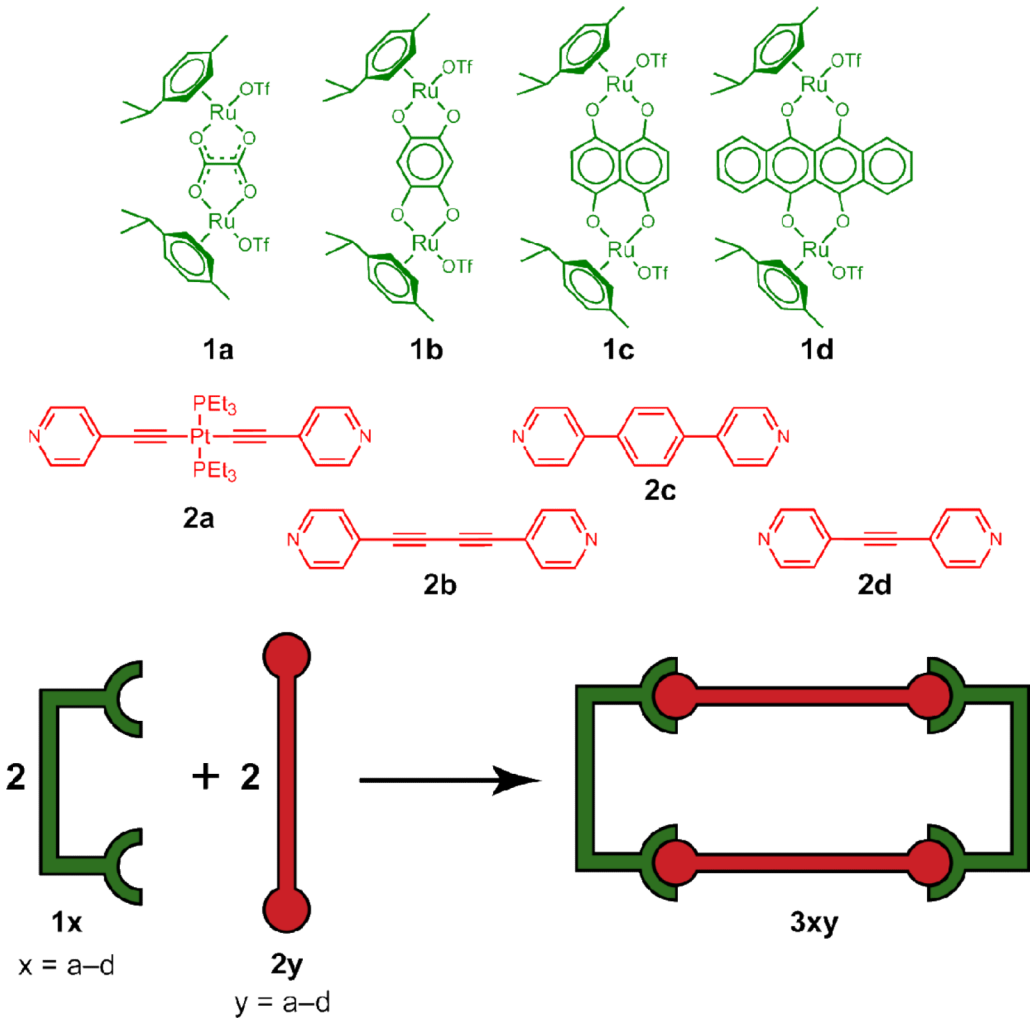

Scheme 1.

Synthetic route to the hetero- and homometallic molecular- rectangles. **1a-d** denote arene-Ru acceptors, **2a-d** denote dipyridyl donors, **3xy** denote metalla-rectangles where x refers to the acceptor and y refers to the donor components used.

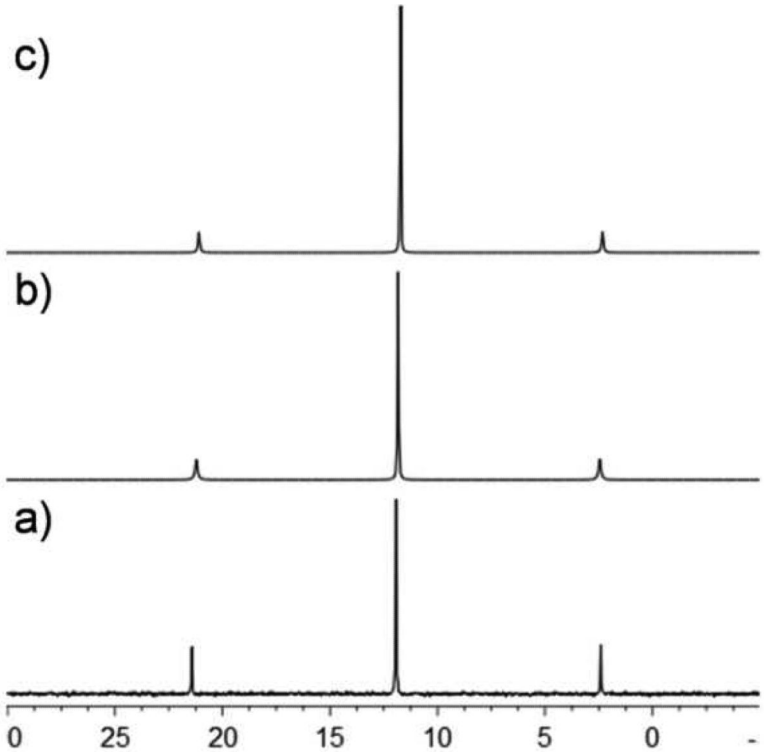

Figure 1.
^{31}P NMR spectra of donor **2a** (a) and heterometallic-rectangles **3ca** (b) and **3da** (c).

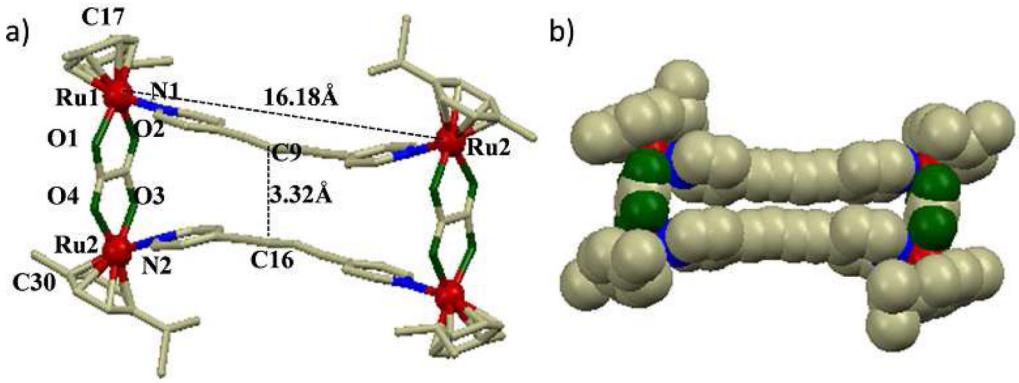

Figure 2.
(a) Numbered diagram of X-ray crystal structure of the molecular rectangle **3ab**; Solvent molecules and hydrogen atoms are omitted for clarity (color codes: red = Ru, green = O, blue = N and gray = C), (b) Space-filling model of **3ab**.

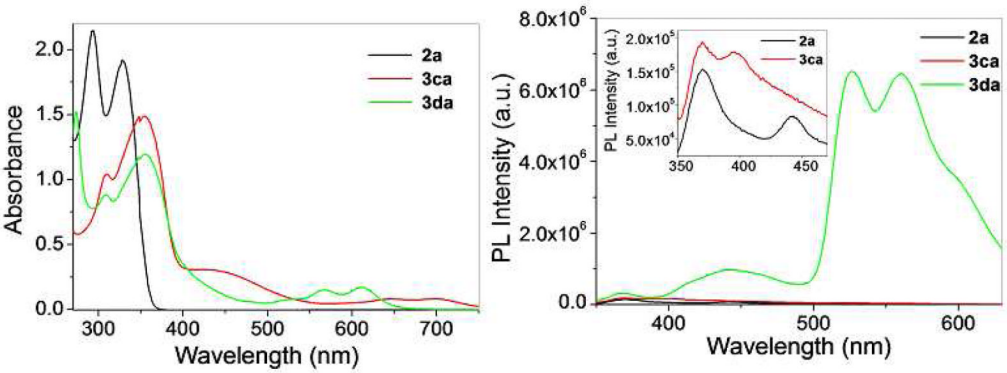

Figure 3.

UV-vis absorption (left) and emission spectra (right, the inset shows the expended view) of Pt-based donor **2a** and heterometallic rectangles **3ca** and **3da**.

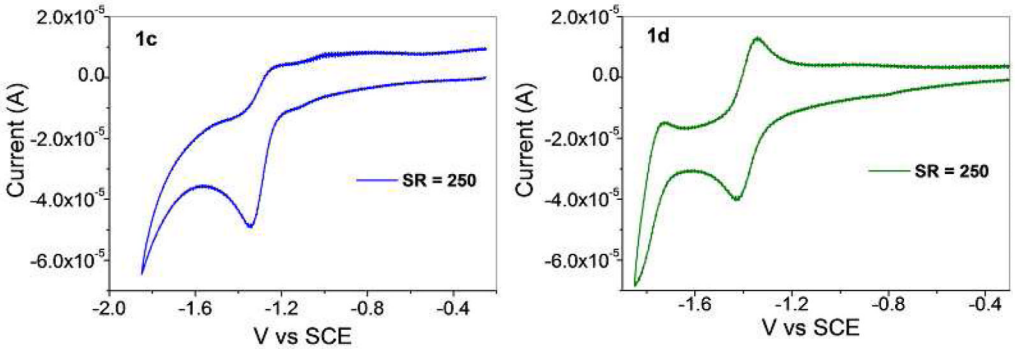

Figure 4.
Cyclic voltammograms of **1c** and **1d** (0.5 mM in CH_2Cl_2 at Pt-disk) at a scan rate 250 mV s^{-1}.

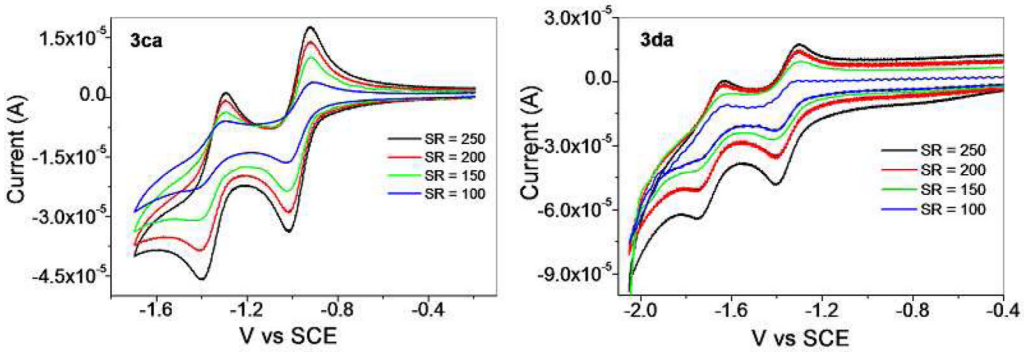

Figure 5.
Cyclic voltammograms of 0.5 mM of **3ca** and **3da** at a scan rate of 100-250 mV s^{-1}.

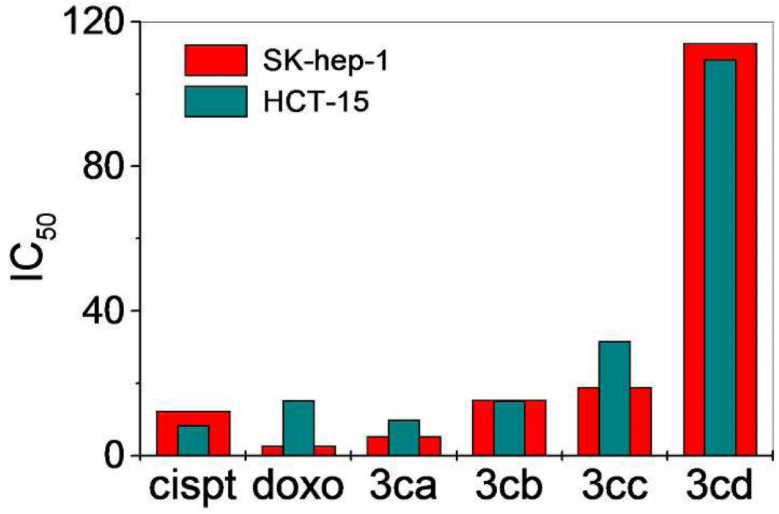

Figure 6.
Comparison of antitumor activity of metalla-rectangles (**3ca**, **3cb**, **3cc** and **3cd**), cisplatin and doxorubicin against SK-hep-1 and HCT-15 human cancer cell lines.

Table 1

Bond lengths [Å] and angles [°] for **3ab**.

Ru(1)-O(2)	2.05(9)	Ru(1)-O(1)	2.08(8)
Ru(1)-N(1)	2.12(5)	Ru(1)-C(17)	2.16(5)
Ru(2)-O(4) #1	2.05(12)	Ru(2)-N(2)	2.09(5)
Ru(2)-O(3) #1	2.12(10)		
O(2)-Ru(1)-O(1)	78.8(4)	O(2)-Ru(1)-N(1)	82.6(2)
O(1)-Ru(1)-N(1)	83.8(2)	O(4)#1-Ru(2)-C(30)	160.2(3)
N(2)#1-Ru(2)-C(30)	114.7(3)	N(2)#1-Ru(1)-C(27)	115.4(3)
O(4) #1-Ru(2)-N(2)	85.0(3)	N(2)-Ru(2)-O(3) #1	85.6(3)

Table 2

Photophysical properties of the metalla-rectangles.

Molecular-rectangle	Absorption maxima λmax(nm) (Molar extinction co-efficient 10^5 ε M^{-1} cm^{-1})	λ_{ex}(nm)	Emission maxima λ_{max}(nm)
3ca	309 (1.09), 352(1.48), 446 (0.29), 639(0.08), 701 (0.08)	330	370, 390
3da	308 (0.86), 355 (1.19), 565 (0.14), 611 (0.18)	330	370, 443, 525, 560
3ab	303 (0.84), 323 (1.00), 337 (0.83)	298	335
3bb	316 (0.95), 358 (0.60), 494 (0.39)	298	335
3cb	323 (0.62), 353 (0.51), 437 (0.21), 643 (0.04), 701 (0.05)	330	370
3ac	312 (0.76)	298	339, 383
3bc	310 (1.25), 494 (0.41)	298	372
3cc	325 (0.61), 353 (0.50), 439 (0.21), 645 (0.05), 701 (0.04)	330	370
3ad	316 (0.48)	298	334, 352
3bd	304 (1.01), 492 (0.43)	298	357, 374
3cd	294 (0.56), 318 (0.49), 435 (0.20), 645 (0.05), 701 (0.05)	330	370

Table 3

Cytotoxicity of the complexes in human cancer cells.

Metalla-rectangle	IC_{50} μM[a]			
	SK-hep-1	HeLa	HCT-15	AGS
3ca	5.36±0.38	9.40±0.51	9.83±0.33	2.65±0.02
3da	8.60±0.65	9.55±0.87	13.27±0.03	10.83±0.30
3ab	51.08±0.95	14.91±0.59	11.40±0.15	9.61±0.55
3bb	58.88±0.08	43.74±2.08	11.91±0.10	10.37±0.69
3cb	15.45±0.95	20.48±2.70	15.23±0.87	11.65±0.16
3ac	>200	>200	>200	>200
3bc	>200	>200	>200	>200
3cc	19.00±4.99	-	31.74±0.25	-
3ad	>200	>200-	>200	>200
3bd	>200	>200	>200	>200
3cd	114.05±2.69	-	109.60±5.49	31.96±2.25
2a	>200	>200	>200	>200
2b	>200	>200	>200	>200
2c	>200	>200	>200	147.0±7.54
2d	178.60±10.05	>200	>200	>200
Cisplatin	12.38±0.24	76.85±0.41	8.38±2.31	>100
Doxorubicin	2.67±0.24	3.16±0.04	15.34±0.58	0.70±0.16

[a] IC_{50}: drug concentration necessary for 50% inhibition of cell viability.